Wiley
International Journal of Energy Research
Volume 2025, Article ID 7974511, 14 pages
https://doi.org/10.1155/er/7974511

WILEY

Research Article

Design and Performance of a Gravity Water Fed In-Duct Crossflow Turbine for Hydropower Generation

Job Kitetu,[1] **Thomas F. N. Thoruwa**,[2] **and Isaiah Omosa**[3]

[1]*Kenyatta University, P.O. Box 43844, Nairobi 00100, Kenya*
[2]*School of Pure and Applied Sciences, Pwani University, P.O. Box 195, Kilifi 80108, Kenya*
[3]*School of Engineering and Technology, Kenyatta University, P.O. Box 43844, Nairobi 00100, Kenya*

Correspondence should be addressed to Job Kitetu; jobmuthini@gmail.com

Received 27 August 2024; Revised 10 April 2025; Accepted 7 August 2025

Academic Editor: Jingshou Liu

In Kenya, 70% of households are connected to the grid; however, the consumption of electricity, among households, has reduced by 30%. To address power accessibility inadequacy, especially in rural areas, and develop an appropriate in-duct hydropower (HP) generation system, several horizontal crossflow turbine prototypes were designed based on the field survey data collected from existing pressurized water supply ducts. An assessment carried on water supply schemes in Makueni County led to gathering and mapping required data that included; pipelines of diameters ranging from 50 to 200 mm, water pipe slopes of lengths ranging from 40 to 800 m, slope elevation heads between 14 and 183 m, and 33 potential HP sites with HP production capacity between 0.59 and 23.63 kilowatts. Various horizontal crossflow turbines were designed, fabricated, and tested for HP generation performance. The designed horizontal crossflow turbine has specifications that include a 0.99 mm diameter (D_o) impeller that rotates clockwise, 12.5 mm blade radius of curvature, 0.7033 turbine efficiency, turbine inner diameter of 30 mm (D30), 10 blades (B10), 100 mm diameter pipe, turbine speed of 2210 revolutions per minute (RPM) and production of 5.92 V at a head of 6 m hence making a turbine designed and designated as D30B10. It provides savings on power cost to the extent that in 7.5 years' time, an institution would have saved enough funds to install a new station. On the basis of these findings, it was concluded that in-duct power generation technology is a promising energy harvesting system for rural communities. HP from ducts provides a paradigm shift to the rural communities' source of energy and its use, hence reducing the use of firewood for cooking, which is at 89% and effectively reducing deforestation. More studies are recommended to prototype a full-scale product of the D30B10 turbine to improve technologies for harnessing HP from existing gravity water ducts.

Keywords: break pressure tank (BPT); crossflow turbine; duct; fabrication and global positioning system (GPS); gravity-fed; in-duct turbine; microhydropower; renewable energy; rural electrification

1. Introduction

The global shift toward renewable energy sources underscores the need for sustainable power generation methods [1]. Renewable energy resources in general and hydropower (HP) in particular have been characterized as benign sources of electrical energy that can have a positive contribution to climate change mitigation [2]. About 22% of the world's electricity production comes from HP installations, many of which are small HP schemes (SHPS), which include small HP (SHP), micro-HP (MHP), and pico-HP (PHP) systems [3]. MHP systems generate electricity by converting the kinetic and potential energy of flowing water into mechanical energy, which is subsequently transformed into electrical energy by a generator [4]. Backed by the abundant water resources, MHP systems present a promising solution for rural electrification in Kenya [5]. However, rural electrification in Kenya faces several challenges, including the high cost of grid extension, unreliable power supply, and limited access to affordable energy. This paper explores the design and

performance of a gravity-fed in-duct horizontal crossflow turbine, focusing on optimizing efficiency and feasibility for MHP installations in rural areas. MHP systems offer a viable alternative, providing decentralized power generation that can be tailored to the specific needs and resources of rural communities [6]. The adoption of efficient and cost-effective HP technologies is crucial to overcoming these challenges and improving the quality of life in rural areas. Water ducts can significantly enhance the efficiency of MHP systems by channeling water flow to turbines with increased velocity. This approach not only optimizes energy conversion but also simplifies the integration of HP systems into existing water infrastructure, making it a cost-effective solution for rural areas [4]. The use of gravity-fed water ducts ensures a constant and reliable water flow, essential for consistent power generation.

HP technology uses the gravitational force of falling or flowing water to generate electricity, hence HP, which is considered a source of energy that has a lower-level output of greenhouse carbon dioxide (CO_2) [7, 8]. Apart from the few large and medium HP schemes operating in Kenya, others comprise of SHPS operating in Kenya as (i) SHP (10–1 mW), (ii) mini HP (1 mW–100 kW), (iii) MHP (100–5 kW) and PHP (<5 kW) [9]. The grid is the main source of electricity, with 25% of households connected to it, while 15.3% of the homes are connected to other types of electricity sources [10]. Supported by the feed-in tariff (FIT) policy, small-scale candidate sites are likely to come up and serve well for the electricity supply to villages, small businesses, and farms [11]. There is a need for pressure management to reduce the incidences of pipeline ruptures and decrease the associated repair costs and disruption of water supply to the customers [12], and the use of devices, such as pressure reducing valves (PRVs) in pipeline networks is the most frequently used technology for pressure management and leakage reduction [13]. The researcher is strongly opined that installation of in-duct turbines could act as PRVs.

Community water supply systems in rural areas are composed of water pipelines with diameters raging from fifty millimeters (50 mm) to two hundred millimeters (200 mm). The rural areas of Makueni County are endowed with community water supply systems running to the settlement areas from the Volcanic Chyulu, Mbooni, Nzaui, and Kilungu hills, and their profiles and designs are available in the Makueni County design Office [14, 15].

Turbines extract energy from the fluid by reducing the flow velocity with little or no pressure reduction as the fluid passes through the turbine rotor [16]. HP turbines can be classified depending on the direction of the rotational axis relative to the water flow direction. Axial flow water turbines (AFWTs) have their axis of rotation parallel to the water stream direction, while other turbines, like cross-flow water turbines (CFWTs), have a rotational axis perpendicular to the flow direction [17]. The advantage of cross-flow turbines is that they can rotate unidirectional even with bidirectional fluid flow. They are particularly suited for low-head, high-flow conditions typical of many Kenyan water sources [18]. Also, their ability to handle varying flow rates and debris-laden water makes them ideal for rural installations [19].

In general, turbines can be classified as high head, medium head, or low head machines [20], and energy is extracted primarily by a pressure drop, and this way the open turbine behaves more like an ultra-low head hydroturbine than a conventional wind turbine [21]. Several studies have been conducted in the past on in-duct turbine development. However, as per Bachant and Wosnik [22], Schlabach et al. [23], Rakesh et al. [24], and Zarei and Fard [25], who focused on spherical and helical turbines, the past developed turbines have been on energy production from large (1000, 600, and 300 mm diameter) water supply and wastewater pipes since 2011 to date. Their research recommendations included performance improvement as the turbine diameter decreases, adapting turbine designs to accommodate various pipe diameters and suggesting further research into making these systems scalable for smaller diameters, undertaking design modifications for pipes down to 300 mm diameter and carrying out further numerical and experimental investigations to better understand the behavior of turbines in pipes of smaller diameters respectively. Thus, there is a consistent recommendation on turbines for smaller diameter pipes and improvement on efficiency, and this informed this study focusing on the development of turbines for ducts of less than 300 mm diameter, and specifically a 100 mm diameter duct.

Unlike open turbines, ducted turbines, which involve directing water through a duct to increase velocity and guide the flow onto the turbine blades, can significantly enhance HP system efficiency. The duct's size and shape are crucial in optimizing turbine performance [26]. By controlling the water flow more precisely, ducted turbines can achieve higher efficiency and more stable power output. Ducted hydrosystems can operate across a wide range of head and flow conditions inside most common piping materials such as steel, ductile iron, concrete, or any material that can be mated with steel pipe [27].

There are several practical advantages in placing a turbine in a duct which include: (i) the duct shades the turbine itself from direct sunlight and debris; (ii) a large duct made of low cost materials can be designed so that the downstream side acts as a diffuser and reduces the downstream pressure, thereby increasing the available pressure drop; (iii) large flow area containing a large amount of energy is concentrated into a smaller area so that a smaller, lower cost turbine can be used for a given power output; and (iv) the duct eliminates tip losses on axial flow turbine blades, improving efficiency [28]. The turbine has blades that are mostly curved around its peripheral edge. Water is then released from the pressure pipe onto the runner and fires through, deflecting off the blades as it runs to the center of the runner. This type of turbine is suitable for a head range of about 2–200 m and rating up to approximately 1 mW [29]

The design of an MHP turbine hinges on several key parameters: water flow rate, water head, turbine type, impellers, number of blades, rotor diameter, overall system efficiency, expected electrical potential power, and material used for assembly and fabrication [21, 30]. These turbine parameters must be carefully considered to optimize the system's performance and cost-effectiveness [31]. In the study, the internal systems of the in-duct HP turbine were based on inline impellers (hydro-spin), to develop a microtubular water turbine with a horizontal axis parallel to the water flow [27].

MHP production requires either an induction or a synchronous generator. However, induction generators are preferred because they (i) can operate at variable speeds with constant frequency, (ii) are available at reasonable prices, and (iii) require less maintenance [32]. When a machine's speed ranges from 0 to 1500 revolutions per minute (RPM), it operates as a motor, but when revolutions are between 1500 and 3000 RPM, it operates as a generator and produces electrical energy [33]. Finally, a suitable induction generator was sized to fit with the designed microhydroturbine.

A complete design procedure of a crossflow turbine involves several steps that mainly include: duct sizing, determination of flow rate, net head, blade spacing, design of turbine runner, number of blades, blade radius of curvature, efficiency, power produced, and turbine speed [34]. These steps were adopted in the research to guide the design of highly efficient crossflow turbine for HP production.

2. Materials and Methods

The study employed a combination of experimental and computational methods to design and evaluate the gravity-fed in-duct horizontal crossflow turbine. The methodology included fluid dynamics simulations, prototype fabrication, and performance testing under various operational conditions. Detailed data collection and analysis ensure the accuracy and reliability of the findings.

2.1. Design of Duct Size. The duct size was optimized to enhance water velocity and flow rate through the turbine. Computational fluid dynamics (CFD) simulations using the MATLAB Simulink package, thus varying blade spacing within a 10 mm diameter duct, were used to analyze different duct geometries as obtained from the field findings and their impact on turbine performance [35]. The goal is to identify a duct design that maximizes energy conversion efficiency while maintaining stable flow conditions. In the study, field survey data from identified Makueni County (Kenya) pressurized water ducts potential sites were used for in-duct HP generation. The ducts were made with a mixture of uPVC class E and galvanized iron (GI) heavy-duty pipes with 75 mm minimum diameter were applied while an average gloss head of 40 m was used. The most important design parameter in this design was the velocity of water along the pipes and ranged between 0.6 and 1.5 m/s. Equation (1) was used to confirm the size of pipes laid in identified potential sites.

$$D_{\text{Pipe}} = D = \sqrt{(4Q/\pi V)}, \tag{1}$$

where D_{Pipe} = inside diameter of the pipe (m), Q = design flow (m^3/s), and V = average velocity in the pipe (m/s) [36]. For the consequent designs of various turbine parts, an operation diameter (D_o) of turbine circular motion was used as an equivalent of the pipe diameter, less 0.0005 m from the pipe inner wall. This effectively made the turbine operational diameter less than the pipe diameter by 0.001 m.

$$D_o = D - 0.001. \tag{2}$$

(Author, 2020)

2.2. Selection and Design of a Suitable Hydroturbine Gravity Fed Water Ducts. The hydroturbine was selected and designed based on specific site conditions, including water flow rate and head as obtained from field data on Makueni County pressurized water ducts, as summarized in Table 1. This involved selecting appropriate materials, blade profiles, and rotor dimensions to achieve optimal efficiency [37]. The design process also considered factors such as ease of fabrication, cost, and maintenance requirements. In this project, a suitable and matching hydroturbine was developed for production of HP based on water ducts of diameter that ranged between 100 and 200 mm. However, the development started with consideration of various pipe diameters, from which 100 mm uPVC pipe was adopted for ease of housing of the fabricated turbine. MATLAB Simulink has successfully been used in design and modeling of crossflow turbines [38]; hence, the researcher used the software to model a crossflow turbine. By application of Matlab Simulink, and use of mathematical formulae developed by Yilmaz et al. [39], flow rate (Q), head loss (H_{tl}), blades spacing (t_b), number of blades (n), blades radius of curvature (r_c), turbine frequency (η_t), and turbine power (P_t) were determined. The sizes of pipes used for the turbine development were those of diameter between 75 and 200 mm guided by the existing pipelines within the area of focus, but concentrated on pipes of diameter (D) 100 mm, which were more available in water schemes serving the rural communities and capable of producing applicable power. By applying Equation (14), thus N (RPM) = 125.6 $H_n^{0.5}/nB_s$) as programed in Matlab Simulink software, various spacings of blades in a 100 mm diameter duct, corresponding to specific turbine speeds, were produced. A maximum blade spacing of 50 mm, thus 0.05 m, was applied and reduced subsequently in 10 equal spaces of 0.005 m. Each set of blade spacing was applied against a specific fixed water head, thus 1, 2, 3, 5, 40, and 100 m. More specific formulae programed using Matlab included eight equations listed and described below, and a flowchart in Figure 1.

2.3. Specific Formulae and Description. The several formulae used for the turbine design are as descried as follows:

i. Calculation of the water flow rate (Q) in m^3/s as follows:

$$Q = V \times A\,, \tag{3}$$

where flow velocity is V (m/s) and duct cross-sectional area is A (m^2). Losses are approximately equal to 6% of gross head, which can also be calculated using Darcy–Weisbach (1845) formula, thus Equation (4) as follows:

Table 1: Potential HP sites and parameters.

Site name along pipeline	Latitude	Longitude	Altitude	Elevation (m)	Cum elevation (m)	Pipe size (mm)	Flow rate (m^3/s)	Power (W)
Manooni_Mandei BPT	−1.94214	37.47432	1504	14	14	225	0.0268	2577
Mandei BPT Stream	−1.94186	37.47605	1434	70	84	225	0.0268	15,504
Kwa Nzomi Stream	−1.94342	37.47862	1412	52	52	225	0.0268	9598
Kwa Nzomi AV	−1.94498	37.48183	1432	20	72	225	0.0268	13,289
Kitulani Stream	−1.95013	37.49169	1474	42	114	225	0.0268	21,041
Kitulani Tank Stream	−1.95603	37.49491	1381	81	81	225	0.0268	14,950
Yumbani BPT	−1.96030	37.49412	1439	−58	23	225	0.0268	4245
Kwa Kinza Stream	−1.96458	37.49454	1310	129	129	225	0.0266	23,632
Utuneni S. Tank	−1.98061	37.48923	1415	−105	24	225	0.0266	4397
Kwa Mutula Market	−1.98611	37.48214	1295	22	22	160	0.0139	2106
Kwa Loko BPT	−1.99881	37.48859	1351	38	38	160	0.0139	3638
Musoma S. Tank	−2.00013	37.48892	1302	49	49	140	0.0101	3408
Musoma S. Tank	−2.00013	37.48892	1302	49	87	110	0.0094	5632
Mulima Dam W. O	−1.63067	37.41562	1686	68	68	225	0.0327	15,314
Mulima P S. Tank	−1.62912	37.41376	1739	−53	15	225	0.0327	3378
Mavindu Wash Out	−1.62403	37.41246	1654	85	85	225	0.0327	19,142
Mavindu V BPT	−1.62192	37.4107	1681	−27	58	225	0.0327	13,062
Mavindu M S. Tank	−1.61685	37.41106	1645	36	36	225	0.0160	3967
Mavindu Strm W. O	−1.61432	37.40764	1574	71	71	160	0.0141	6895
Tulimani Road BPT	−1.60224	37.42623	1462	112	183	110	0.0050	6302
Kalawani S. Tank	−1.59477	37.43689	1410	52	52	160	0.0157	5623
Kwa Aithi S. Tank	−1.60835	37.41679	1590	55	55	140	0.0066	2500
Iko_isyu Stream	−1.63313	37.45315	1763	17	17	110	0.0050	585
Nzaini	−1.62300	37.45586	1742	21	38	110	0.0050	1309
Uthuini	−1.62272	37.45647	1728	14	52	110	0.0050	1791
Ikokani Intake	−1.61952	37.45612	1717	11	63	110	0.0050	2169
Factory S. Tank	−1.61779	37.45618	1711	6	69	110	0.0050	2376
Uuta S. Tank	−1.60540	37.46256	1647	64	64	90	0.0050	2204
Kyalya BPT	−1.58889	37.46555	1603	44	108	90	0.0050	3719
Malaa S. Tank	−1.58567	37.46896	1588	25	133	90	0.0050	4580
Kweleli_Ngangani tank	−1.88732	37.55162	1563	83	83	110	0.0050	2858
Yiuma Shrubs BPT	−1.88645	37.55406	1450	113	113	90	0.0050	3891
Yiuma Pr. BPT	−1.88651	37.55629	1379	71	71	90	0.0050	2445

ii. Calculation of total head loss as follows:

$$H_{tl} = 0.0826\, fLQ^2 / D^5\,, \tag{4}$$

where H_{tl} = head loss (m), f = Darcy friction factor (unitless), L = pipe length (m), D = inside pipe diameter (m), and Q = volumetric flow rate (m^3/s).

iii. Calculation of the net head (H_n) as follows:

$$H_n\,(\mathrm{m}) = H_g - H_t, \tag{5}$$

where H_g = the gross head, which is the vertical distance between water surface level at the intake/source and at the turbine, H_t = total head losses due to friction and gate valves, and H is the gross slope head [39].

iv. Calculation of duct diameter (D_o), where N is the turbine speed in RPM as follows:

$$D_o(\mathrm{m}) = 40\sqrt{(H_n)/N}. \tag{6}$$

v. Calculation of the blade spacing (t_b) as follows:

$$t_b = 0.174 \times D_o\,, \tag{7}$$

where D_o is runner outer diameter and t_b is blade spacing.

vi. Calculation of the runner blade number (n): the number of the runner blades was determined as follows:

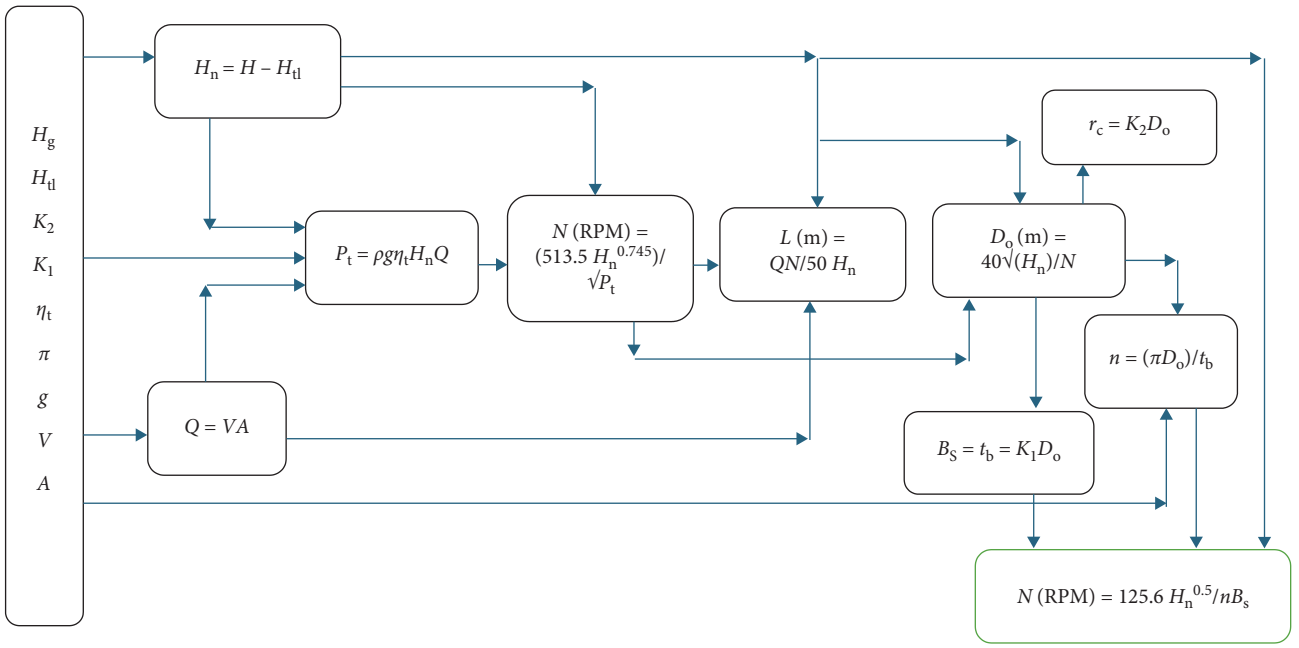

FIGURE 1: Simulation and design flowchart.

$$n = (\pi \times D_o)/t_b. \tag{8}$$

vii. Calculation of the radius blade curvature (r_c) as follows:

$$r_c = 0.126 \times D_o\,. \tag{9}$$

viii. Calculation of turbine efficiency (η_t). The maximum turbine efficiency was calculated as follows:

$$\eta_t = 1/2 \times C^2 \times (1 + \psi) \times \cos^2(\alpha), \tag{10}$$

where ψ is nozzle friction constant, and C is friction on blades constant, and they should be close to unity. Angle (α) should be kept as small as possible for maximum turbine efficiency approximately 16° [40].

ix. Calculation of turbine power (P_t). The electrical power of the turbine in Watts was calculated as follows:

$$P_t = \rho\, g\, \eta_t\, H_n\, Q, \tag{11}$$

where P_t = electrical or mechanical power produced in Watts (W), ρ = density of water (kg/m^3), g = acceleration due to gravity (m/s^2), H = elevation head of water (m), Q = flow rate of water (m^3/s), and η_t = overall efficiency of MHPS [41].

By combining Equations (6) and (11), Equation (12) was produced and programed using Matlab Simulink to establish the relationship between the turbine speed (N), net head (H_n), and flow rate (Q).

$$N(\text{RPM}) = (513.5 H_n 0.25)/\sqrt{\rho\, g\, \eta_t\, Q}\,. \tag{12}$$

(Author, 2020)

By replacing blade spacing (t_b) with (B_s) and using Equations (6)–Equation (8), thus D_o (m) = $40\sqrt{(H_n)}/N$, $t_b = 0.174 D_o$, and $n = (\pi D_o)/t_b$, respectively. A relationship between the blades spacing (B_s), net head (H_n), number of blades (n), and turbine speed (N [RPM]) was developed in Equation (13) as follows:

$$N(\text{RPM}) = \pi \times 40\sqrt{(H_n)/nB_s}. \tag{13}$$

(Author, 2020)

Since π was a nonvarying constant with a known value, Equation (13) was simplified further to Equation (14), which was also programed using Matlab Simulink to provide turbine speed in RPM as follows:

$$N(\text{RPM}) = 125.6\, H_n^{0.5}\,/nB_s. \tag{14}$$

(Author, 2020)

The application of the formulae through Matlab Simulink provided various programing outputs. The researcher adopted a turbine for a 100 mm diameter pipe considering the most available duct sizes in within Makueni County community and production of economically viable power, and an eight blades turbine for initial tests. Guided by all the described steps, a horizontal crossflow turbine whose blades are rotated anticlockwise from the bottom was fabricated.

The final step was the sizing of a suitable generator using Equation (15) as follows:

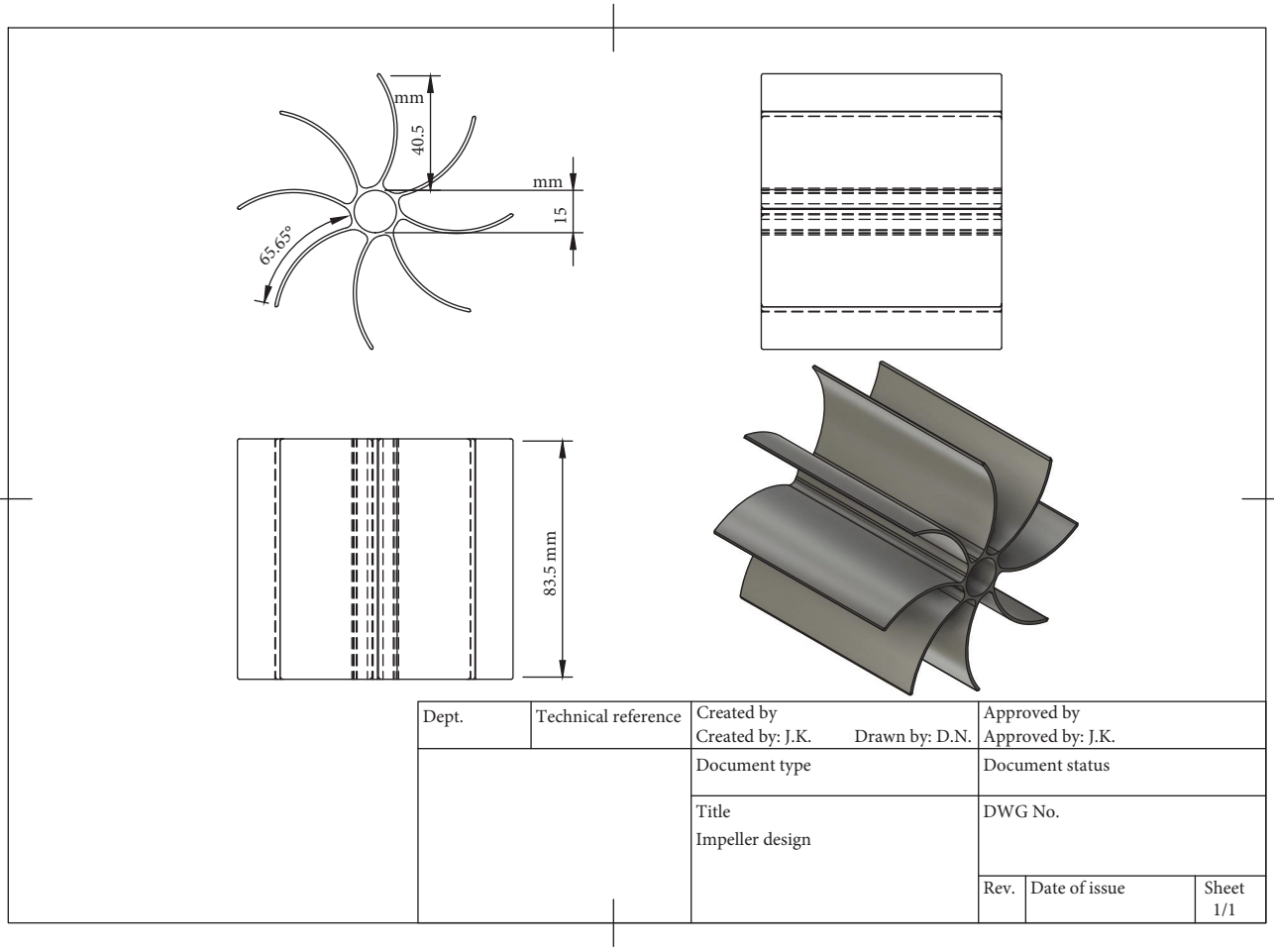

FIGURE 2: Impeller drawing for a designed 15 mm diameter runner.

$$N = 120f/p, \tag{15}$$

where N *is* the number of RPM, f is system frequency, while p represents the generator poles [42].

2.4. Fabrication of an Appropriate Turbine. The fabrication process included manufacturing turbine components and assembling the system for testing. Precision in fabrication is crucial to ensure efficient and reliable turbine operation [43]. The materials and manufacturing techniques were selected to ensure durability and performance in rural environments. A GI plain sheet of 0.8 mm thickness was welded to make a turbine housing of 1 m long by 100 mm diameter pipe-like oral structure with symmetrical holes to hold the turbine shaft in a horizontal position.

Several turbine impellers were designed and developed using additive manufacturing, thus creating a three-dimensional (3D) object layer-by-layer using a computer-aided design [44]. Considering that there are several varieties of 3D printing materials, including thermoplastics such as acrylonitrile butadiene styrene (ABS), metals (including powders), resins, ceramics, and thermoplastics, a thermoplastic polyester material was used to develop various turbines using material extrusion, thus fused deposition modeling (FDM). It is cheaper and provides the minimum structural integrity required for this project. Polylactide (PLA) is also the safest material to use in your 3D Printer. It is made from entirely natural substances such as maize and sugarcane. When it is heated, PLA gives off a nontoxic chemical called lactide. Moreover, it is rated food safe and can be used in applications surrounding water [45].

The ratio of inner (R_2) and outer (R_1) diameters of turbine runner is 0.66, and the number of blades is 18. Fewer blades may cause pulsating power, while a large number of blades may cause excessive frictional loss, and therefore, the optimum number can be found by experiment [40]. The research focused on an in-duct turbine design, hence various turbine impellers were designed and produced with inner runner diameters of 15, 30, and 65 mm and blades varying from 5 to 18. Figure 2 shows a drawing of designed impeller on 15 mm diameter runner, and Figure 3 contains design and performance plates. Plate 3.3 shows the designed impeller, while the specifications of the designed and adopted turbine on a 30 mm diameter runner are summarized in Table 2.

The various turbine impellers were fixed in the fabricated turbine housing, connected to the installed pipeline, and with the use of a tachometer, the RPM under 100 mm diameter pipe

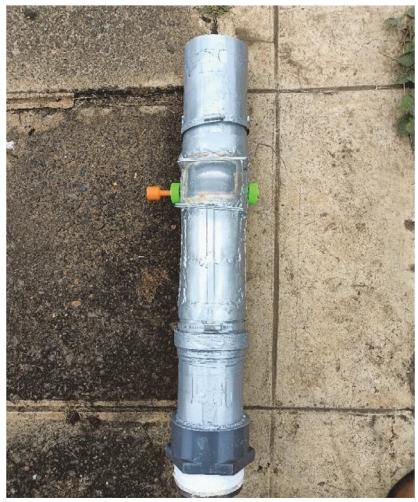

Plate 3.1: Fabricated turbine assembly

Plate 3.2: Turbine impeller in position

Plate 3.3: Weighing impeller

Plate 3.4: Reading RPM values using a tachometer

FIGURE 3: Design and performance photos.

TABLE 2: RPM for various numbers of blades and runner diameters.

Number of blades	D15, 4" max RPM	D30, 4" max RPM	D65, 4" max RPM
8	14.61	14.16	—
10	**10.89**	**22.01**	**8.63**
12	10.10	21.20	6.86
15	9.98	16.74	8.26
18	9.98	12.21	7.43

Note: All across, as highlighted, the 10 blades produced the highest speeds (the RPM values were reduced at a ratio of 1:100).

were measured and recorded for analysis as shown in Plate 3.4. The final testing assembly with the fabricated turbine is as shown in Plates 3.1 and 3.2.

2.5. Optimization of Turbine RPM, Voltage, and Current. A testing site was set at Kenyatta University Appropriate Technology Center (KUATC), as shown in Figure 4. Instrumentation involved the use of sensors and data acquisition systems to measure turbine performance parameters such as water flow rate, turbine RPM (Laser Photo/Contact Tachometer-RPM33-China), voltage, and current (Digital Multimeter, model 1009-Japan). Data analysis included processing the collected data to evaluate the efficiency, power output, and operational stability of the turbine. Statistical methods (an Excel package) and computational tools (Matlab Simulink-2020) were employed to ensure robust analysis and interpretation of results.

3. Results and Discussion

Section 3 presents results and discussion on designed turbine guided by pipeline data collected in the field, along the water pipelines on potential HP sites, as shown in Table 1. Also included are performance and parameters that include blade spacing, the RPM, voltage, and power produced.

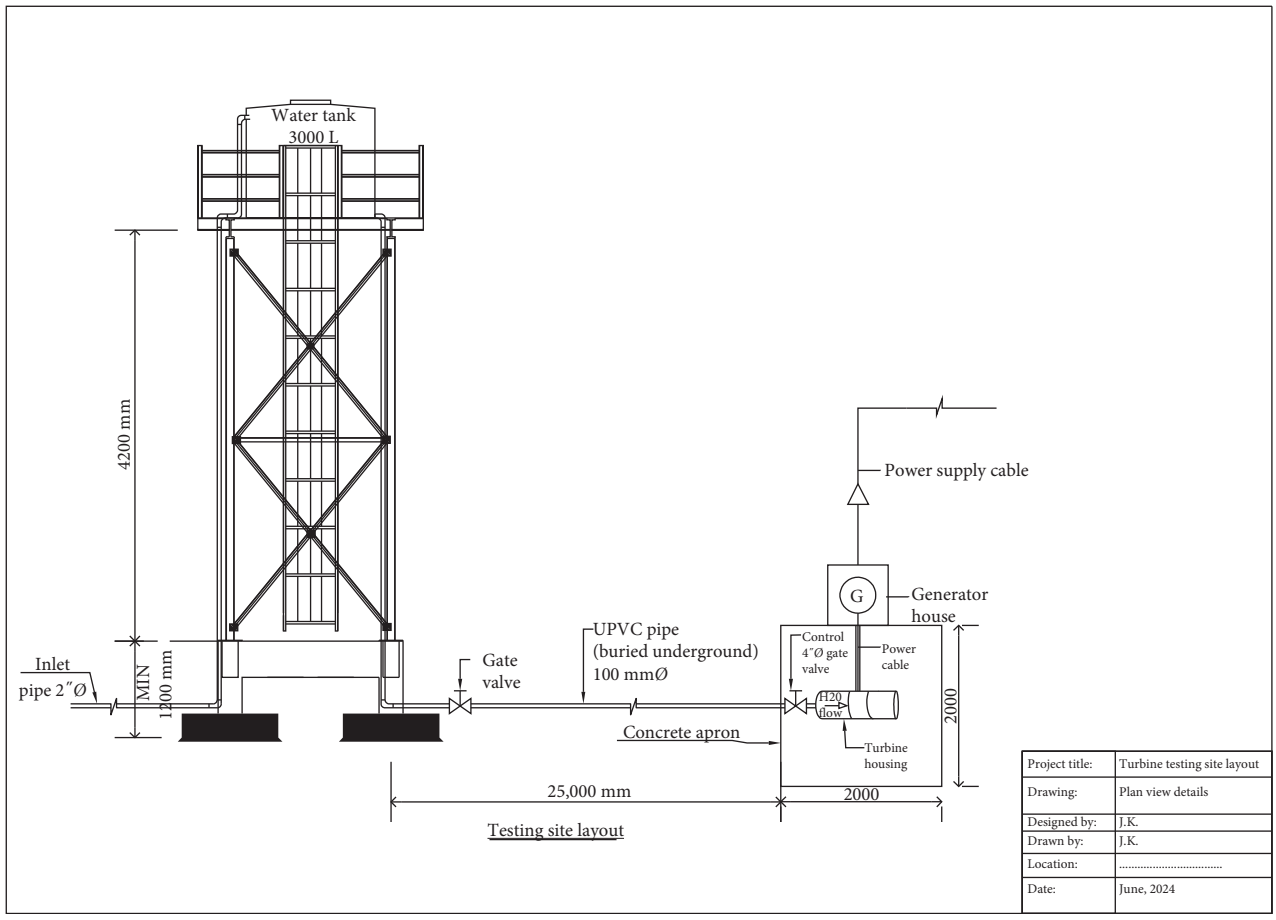

Figure 4: Turbine testing site layout.

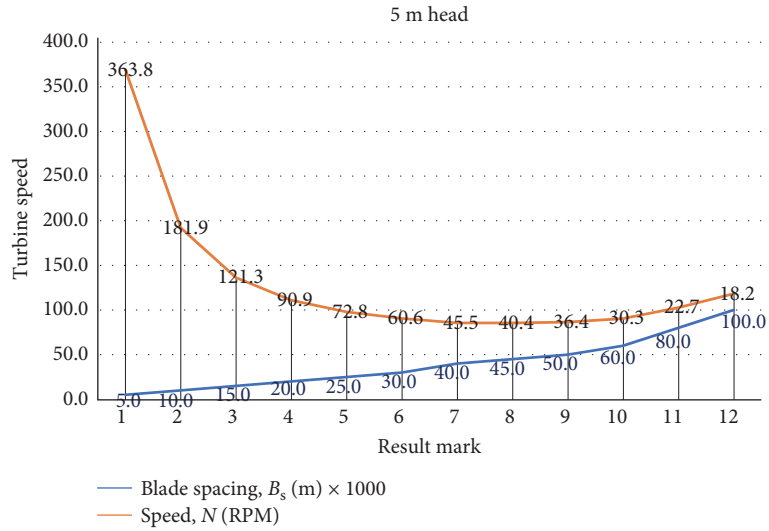

Figure 5: Speed and spacing for 5 m head.

3.1. Turbine Design. Design of the turbine was undertaken with a focus on the key parameters that included the number of blades (n), the blades spacing (B_s), and turbine speeds/RPM. For the production of clear graphs, the spacing values were increased, with a factor of 10^3. The graphs for blade spacing versus speed (Figures 5 and 6) produced similar curves in which the speed increased gradually as spacing decreased from 0.1 to 0.02 m. From a blade spacing of 0.02 m, the curves

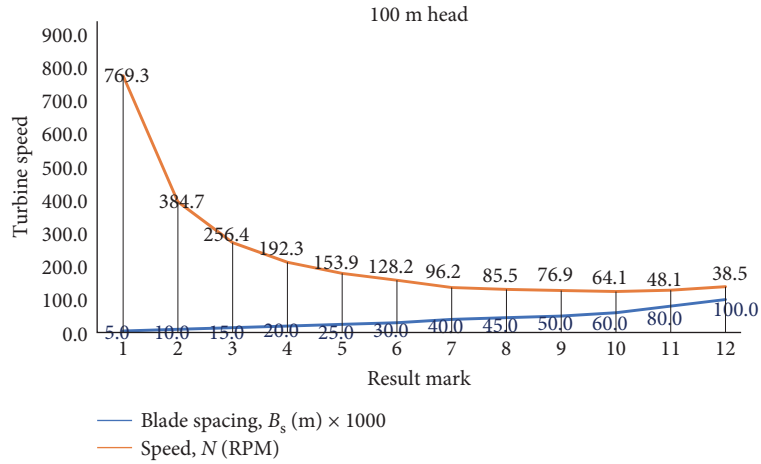

Figure 6: Speed and spacing for 100 m head.

Table 3: Blades and blade spacing values.

Item	Values											
Blade spacing, B_s (m) × 100	0.5	1.0	1.5	2.0	2.5	3.0	4.0	4.5	5.0	6.0	8.0	10.0
Number of blades ($n = P_i \times D_{bc}/B_s$)	62.2	31.1	20.7	15.5	12.4	10.4	7.8	6.9	6.2	5.2	3.9	3.1

Note: D_{bc} is the diameter of blade circumference inside a duct.

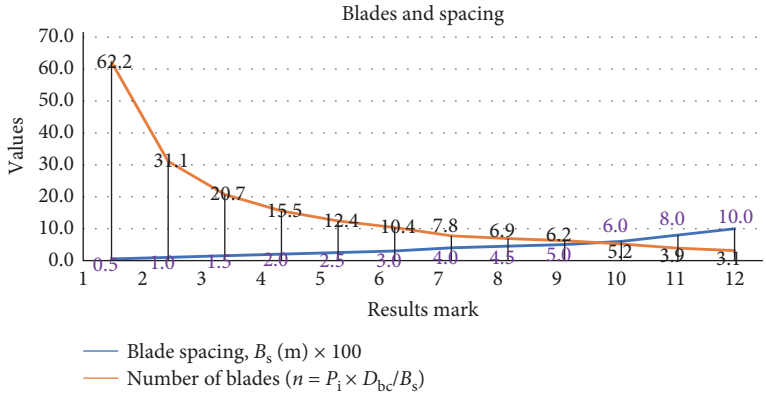

Figure 7: Blades and spacing.

started depicting a sharp rise with the smallest blade spacing of 0.005 m. This confirmed that 18 is the maximum number of blades, but the optimum number can be found by experiment [40]. The blades spacing (B_s) at the pipe wall side is indirectly proportional to the number of blades (n), thus the number of blades (n) = pipe circumference/blade spacing.

Using the MATLAB Simulink-generated information as shown in Table 3 and Figure 7, the researcher made further conclusions toward the best number of blades to start the experimentation. The blades curve in Figure 7 showed a gradual increment value between 5.2 and 6.9, thus 5–7 blades. By considering the average blades' range (5–7), the researcher selected six blades as the minimum number of turbine blades for further design process. This decision was finally confirmed by the experiments in which 10 blades (for all the experimented turbine runners of diameters D15, D30, and D65) depicted the highest RPM, voltage, and current as shown in Figure 8.

To determine the other turbine parameters, the effective turbine diameter (D_o) was used in the research Equation (2); thus, $D_o = D - 0.001$ was applied and resulted to, $D_o = 0.1 - 0.001 = 0.099$ m = 99 mm.

The blade's radius of curvature significantly affected turbine efficiency. The blade's radius of curvature (r_c) was determined using Equation (9), thus $r_c = 0.126 \times D_o = 0.126 \times 99 = 12.5$ mm.

Experimental results indicate that a smaller radius of curvature improves the turbine's ability to harness the kinetic energy of water flow [46]. This design consideration is critical for maximizing energy conversion efficiency. The overall turbine efficiency was assessed by measuring power output relative to the theoretical potential energy of the water. The optimized design achieves an efficiency of ~70%, comparable to other MHP systems [4]. These efficiency gains are essential for making MHP a viable option for rural electrification. The designed

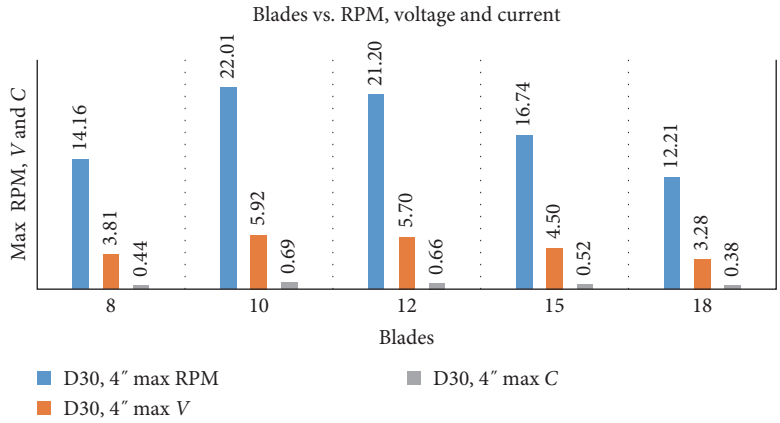

Figure 8: D30B10 RPM, voltage, and current values.

Table 4: RPM, voltage, and current for various numbers of blades and 30 mm diameter runner.

Number of turbines	D30, 4" max RPM	D30, 4" Max *V*	D30, 4" Max *C*
8	14.16	3.81	0.44
10	**22.01**	**5.92**	**0.69**
12	21.20	5.70	0.66
15	16.74	4.50	0.52
18	12.21	3.28	0.38

Note: All across, as highlighted, the 10 blades produced the highest speeds (the RPM values were reduced at a ratio of 1:100), voltage and current values.

turbine efficiency was determined using Equation (10); $\eta_t = 1/2C^2(1+\psi)\cos^2(\alpha)$, where C (blade roughness), ψ (nozzle roughness) coefficients which should be close to unity, and α (attack angle) were estimated as 0.98° and 16° [40].

However, the attack angle in the experiment varied between 17° and 21° hence an average of 19° was adopted, while the roughness was between 05 and 1, hence an average of 0.90 constant value was used in the experiment for the thermoplastic blades.

Therefore $\eta_t = ½ \times 0.90^2 \times (1+0.90) \times \cos^2(19)$

$= 0.5 \times 0.81 \times 1.9 \times \cos^2(19) = 0.5 \times 0.81 \times 1.9 \times 0.914$, thus $\eta_t = 0.7033$.

3.2. Optimization of Turbine RPM, Voltage, and Current. The turbine's rotational speed (RPM) was optimized to match the generator's operating characteristics, ensuring maximum power output and minimal mechanical losses [47]. Proper RPM optimization is crucial for achieving consistent and reliable power generation. In this research, the ratio of inner (R_2) and outer (R_1) diameters of turbine runner was 0.66, and the highest number of blades was 18, but the optimum number was found by experiment [40], and the design from Matlab simulation in Figure 7 settled on an average of six blades. However, bearing in mind that the research focused on a 100 mm (4") diameter induct turbine design, various turbines were designed and produced with inner runner diameters of 15, 30, and 65 mm and blades varying from 5 to 20 but those which produced tangible results were blades from 8 to 18. Several performance graphs for various numbers of blades versus various turbine runner diameters were developed, as shown in Tables 2 and 4, Figures 9 and 8. The results demonstrated stable and consistent power generation, suitable for rural electrification and small-scale applications [48]. This stability is vital for ensuring reliable power supply to rural communities. The results are presented in Figure 10. The optimization of turbine RPM, Voltage and Current produced various results as shown in Tables 2 and 4 and also in Figures 9 and 8 where after all the various speed, voltage and current values for turbines with 8, 10, 12, 15 and 18 blades were recorded and analyzed, the turbine of inner diameter of 30 mm and 10 blades (D30B10) for a 100 mm diameter duct provided the highest RPM of 2210 and power of 5.92 V at a head of 6 m. Therefore, the D30B10 turbine was experimentally selected as the best performing. The effect on water flow rate was the lowest (40.1% reduction) for a 10-blade impeller on a 30 mm diameter runner (D30B10), as shown in Figure 11, with the highest flow rate of 20.74×10^{-4} m^3/s, hence confirming the selection of the turbine as the best. The specifications of the designed turbine are summarized in Table 5.

The D30B10 turbine for a 100 mm diameter duct, as shown in Figure 10, produced lighting by connecting a 6-volt dynamo assembled with a lighting bulb at the KUATC testing site.

The turbine's electrical output in terms of voltage and current was measured and presented in triplicate. The results demonstrate stable and consistent power generation, suitable for rural electrification and small-scale applications [48]. This stability is vital for ensuring reliable power supply to rural communities. The results are presented in Figure 10.

3.3. Conclusion. Optimized design parameters result in high efficiency and reliable performance, hence the gravity-fed induct horizontal crossflow turbine shows substantial potential for MHP generation in Kenya.

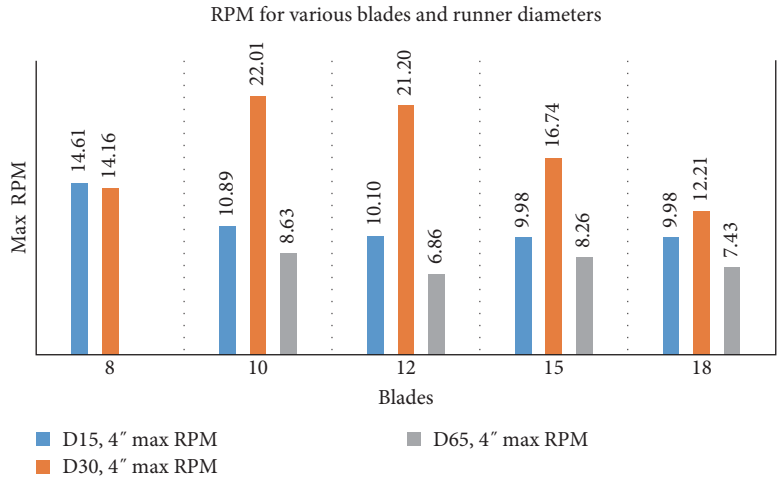

Figure 9: RPM values for runner D15, D30, and D65.

Figure 10: Demonstration of lighting by in-duct turbine at testing site in KUATC.

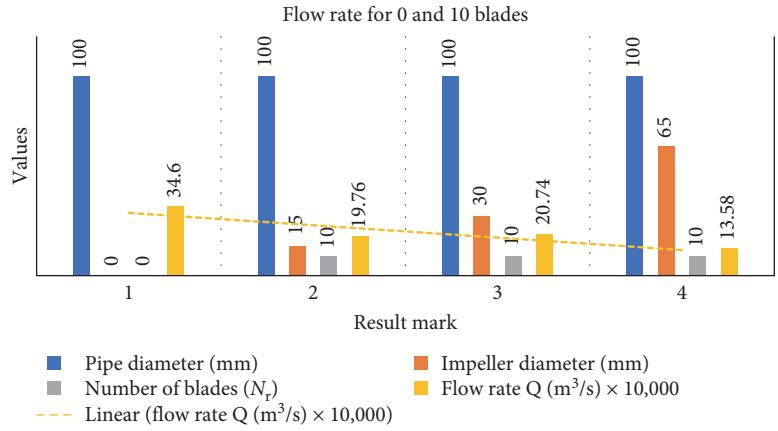

Figure 11: Flow rates for 0 and 10 blades.

The findings highlight the viability of utilizing gravity-fed water ducts for HP generation in rural areas. The study's implications suggest that gravity-fed water ducts can be effectively utilized for HP generation in Kenya, providing a sustainable and cost-effective energy solution for rural communities.

Consequently, this will facilitate opening of community members' minds to business development, hence making the communities and institutions in the rural areas venture into income-generating activities like rearing of poultry and development of light industries, including grinding of maize and other cereals. This approach can significantly contribute to rural electrification efforts and reduce dependance on nonrenewable energy sources.

The successful implementation of such a system enhances energy security in rural areas, provides a paradigm shift to the rural communities' source of energy, improves the quality of

Table 5: Specifications of final designed and adopted hydroturbine.

Item	Research	Result
1	Duct diameter for experiment	100 mm
2	Turbine housing diameter	100 mm
3	Turbine housing length	1000 mm
4	Runner diameter (D)	30 mm
5	Number of blades (B)	10
6	Blade radius of curvature (r_c)	12.5 mm
7	Designed turbine efficiency (η_t)	0.7033
8	Turbine designated name	D30B10
9	Turbine housing average flow rate (FR)	0.00346 m^3/s
10	Average FR with impeller in turbine housing	0.00207 m^3/s
11	Reduction of FR due to Impeller	40.1%
12	Highest revolutions@6 m head	2210 RPM
13	Highest voltage@6 m head	5.92 V
14	Cost-saving time for an in-duct hydropower turbine replacement	7.5 years

life, reduces the use of firewood for cooking, which is at 89% in Makueni County, and effectively reduces deforestation, environmental degradation, and promote economic development.

Further implications of implementing the designed HP system are assisting in breaking pressure along the pipelines by acting as break pressure tanks (BPTs), hence significantly reducing the costs associated with repairing burst pipelines.

Due to the low cost of paying for power associated with the designed system, LCCA conducted on the system revealed that the savings on power is such a feasible phenomenon that in 5.5 years' time, an institution will have saved enough funds to install a new station or replace the one that has been in existence.

3.4. Recommendations. The designed and tested turbine of inner diameter of 30 mm and 10 blades (D30B10) for a 100 mm diameter pipe is recommended as the best to inform further designs and research on in-duct turbines including pipes smaller pipes.

Further research is recommended to explore the long-term durability of the turbine and its scalability for larger installations.

Data Availability Statement

The authors confirm that the data supporting the findings of this study are available within the article. Also, upon request, data are available from the corresponding author (Job Kitetu).

Conflicts of Interest

The authors declare no conflicts of interest.

Funding

No funding was received for this manuscript.

References

[1] Q. Hassan, P. Viktor, T. J. Al-Musawi, et al., "The Renewable Energy Role in the Global Energy Transformations," *Renewable Energy Focus* 48 (2024): 100545.

[2] R. Siri, S. R. Mondal, and S. Das, "Hydropower: A Renewable Energy Resource for Sustainability in Terms of Climate Change and Environmental Protection," in *Alternative Energy Resources: The Way to a Sustainable Modern Society*, 99, (Springer, 2021): 93–113.

[3] E. F. Moran, M. C. Lopez, N. Moore, N. Müller, and D. W. Hyndman, "Sustainable Hydropower in the 21st Century," *Proceedings of the National Academy of Sciences* 115, no. 47 (2018): 11891–11898.

[4] P. Gokhale, A. Date, A. Akbarzadeh, et al., "A Review on Micro Hydropower in Indonesia," *Energy Procedia* 110 (2017): 316–321.

[5] S. J. Chemengich and D. O. Masara, "The State of Renewable Energy in Kenya With a Focus on the Future of Hydropower," *Africa Environmental Review Journal* 5, no. 1 (2022): 246–260.

[6] World Bank, *Kenya: Off-Grid Solar Access Project for Underserved Counties* (World Bank Project Paper, 2019).

[7] S. O. Anaza, M. S. Abdulazeez, Y. A. Yisah, Y. O. Yusuf, B. U. Salawu, and S. U. Momoh, "Micro Hydro-Electric Energy Generation—An Overview," *American Journal of Engineering Research (AJER)* 6, no. 2 (2017): 5–12.

[8] Y. Bayazıt, "The Effect of Hydroelectric Power Plants on the Carbon Emission: An Example of Gokcekaya Dam, Turkey," *Renewable Energy* 170 (2021): 181–187.

[9] J. N. Shrestha, K. A. Techato, W. Khongnakorn, S. Gyewali, and M. R. Dangal, "Hydropower-Renewable Energy Solution for Sustainable Development: A Review of Hydropower Development in Nepal," *Water and Energy International* 65, no. 1 (2022): 44–52.

[10] A. George, S. Boxiong, M. Arowo, P. Ndolo, Chepsaigutt-Chebet, and J. Shimmon, "Review of Solar Energy Development in Kenya: Opportunities and Challenges," *Renewable Energy Focus* 29 (2019): 123–140.

[11] S. W. Ndiritu and M. K. Engola, "The Effectiveness of Feed-in-Tariff Policy in Promoting Power Generation From

Renewable Energy in Kenya," *Renewable Energy* 161 (2020): 593–605.
[12] N. Samir, R. Kansoh, W. Elbarki, and A. Fleifle, "Pressure Control for Minimizing Leakage in Water Distribution Systems," *Alexandria Engineering Journal* 56, no. 4 (2017): 601–612.
[13] T. C. Mosetlhe, Y. Hamam, S. Du, and E. Monacelli, "A Survey of Pressure Control Approaches in Water Supply Systems," *Water* 12, no. 6 (2020): 1732.
[14] Makueni County Government, "Makueni County Integrated Development Plan (CIDP): Makueni County Government," (2018).
[15] J. M. Kitetu, T. Thoruwa, and I. B. Omosa, "Potential of In-Duct Hydropower Generation in Makueni County," *International Journal of Engineering Research & Technology (IJERT)* 12, no. 8 (2023): 1–6.
[16] Z. Yuan, Q. Zheng, G. Yue, and Y. Jiang, "Performance Evaluation on Radial Turbines With Potential Working Fluids for Space Closed Brayton Cycle," *Energy Conversion and Management* 243 (2021): 114368.
[17] R. Gosselin, G. Dumas, and M. Boudreau, "Parametric Study of H-Darrieus Vertical-Axis Turbines Using CFD Simulations," *Journal of Renewable and Sustainable Energy* 8, no. 5 (2016).
[18] M. Elgammi and A. A. Hamad, "A Feasibility Study of Operating a Low Static Pressure Head Micro Pelton Turbine Based on Water Hammer Phenomenon," *Renewable Energy* 195 (2022): 1–16.
[19] L. Mbele, "Utilization of Small Conduit Hydropower Generation for Domestic Loads," (2019).
[20] N. F. Yah, A. N. Oumer, and M. S. Idris, "Small Scale Hydro-Power as a Source of Renewable Energy in Malaysia: A Review," *Renewable and Sustainable Energy Reviews* 72 (2017): 228–239.
[21] E. Quaranta, M. Bonjean, D. Cuvato, et al., "Hydropower Case Study Collection: Innovative Low Head and Ecologically Improved Turbines, Hydropower in Existing Infrastructures, Hydropeaking Reduction, Digitalization and Governing Systems," *Sustainability* 12, no. 21 (2020): 8873.
[22] P. Bachant and M. Wosnik, "Experimental investigation of Helical Cross-Flow Axis Hydrokinetic Turbines, Including Effects of Waves and Turbulence," in *Fluids Engineering Division Summer Meeting*, 44403, (ASME, 2011): 1895–1906.
[23] R. Schlabach, J. Thomas, N. Weaverdyck, and M. C. Johnson, "Lucid Energy Inc." in *In-Conduit Hydropower*, (Lucid Energy Inc., 2013).
[24] C. Rakesh, C. Nallode, M. Adhvaith, T. J. Anwin, A. A. Krishna, and C. Rakesh, "Theoretical Study and Performance Test of Lucid Spherical Turbine," *International Journal for Innovative Research in Science and Technology* 3 (2016): 418–423.
[25] H. Zarei and M. P. Fard, "Numerical Investigation of Lucid Spherical Cross-Axis Flow Turbine With Asymmetric Airfoil Sections and the Effect of Different Parameters of Blades on Its Performance," *Journal of Applied Fluid Mechanics* 17, no. 1 (2023): 176–191.
[26] M. M. Rahman, A. A. Bhuiyan, and M. Kamruzzaman, "Impact of Ducted Turbine Design on Micro-Hydropower Efficiency," *Renewable Energy* 93 (2016): 168–175.
[27] C. Marco, "Harvesting Energy From in-Pipe Hydro Power Systems in Urban and Building Scale," *International Journal of Smart Grid and Clean Energy* 4, no. 4 (2015): 316–327.
[28] T. T. Rajaonary, *Design and Optimization of a Hydrokinetic Turbine Duct With CFD*, (Master's thesis, Fen Bilimleri Enstitüsü, 2016).
[29] R. Prophet, *An Investigation Into the Feasibility of a Micro-Hydro Installation for the Guard Bridge Energy Centre as Part of a Brownfield Redevelopment* (University of University of Strathclyde, 2015).
[30] H. A. Mrope, Y. A. Chande Jande, and T. T. Kivevele, "A Review on Computational Fluid Dynamics Applications in the Design and Optimization of Crossflow Hydro Turbines," *Journal of Renewable Energy* 2021 (2021): 5570848.
[31] T. Coda, K. Gupta, and J. Robbins, "Micro-Hydro Power Potential for Caroline, NY: A Feasibility Study," (2017).
[32] K. Subramanya and T. R. Chelliah, "Capability of Synchronous and Asynchronous Hydropower Generating Systems: A Comprehensive Study," *Renewable and Sustainable Energy Reviews* 188 (2023): 113863.
[33] M. A. Özçelik, "Operating the Induction Motor as a Generator Mode by Supplying DC Voltage and Investigation of the End Voltage Depending on the Excitation Current and RPM," *International Journal of Energy Research* 2023 (2023): 9967218.
[34] A. Bilal, "Design of High Efficiency Crossflow Turbine for Hydro-Power Plant," *International Journal of Engineering and Advanced Technology (IJEAT)* 2, no. 3 (2013): 308–311.
[35] T. L. Oladosu and O. A. Koya, "Numerical Analysis of Lift-Based in-Pipe Turbine for Predicting Hydropower Harnessing Potential in Selected Water Distribution Networks for Waterlines Optimization," *Engineering Science and Technology, An International Journal* 21, no. 4 (2018): 672–678.
[36] J. Toteff and M. A. Tovar, "Design and Multiparameter Optimization of Jet-Pumps in a Pipeline Loops Using CFD Tools," in *Proceedings of the ASME 2018 5th Joint US-European Fluids Engineering Division Summer Meeting*, (American Society of Mechanical Engineers, 2018).
[37] P. Singh, F. Nestmann, and A. Alvarado, "Design Optimization of Micro Hydro Turbines," *Renewable Energy* 83 (2015): 1046–1056.
[38] R. C. Adhikari and D. H. Wood, "Computational Analysis of Part-Load Flow Control for Crossflow Hydro-Turbines," *Energy for Sustainable Development* 45 (2018): 38–45.
[39] A. Yilmaz, A. Oguz, and Y. Celal, "A Sensitivity Analysis for the Design of Small-Scale Hydropower Plant: Kayabogazi Case Study," *Renewable Energy* 33 (2008): 791–801.
[40] D. H. Ngoma, Y. Wang, and T. Roskilly, "Crossflow Turbine Design Specifications for Hhaynu Micro-Hydropower Plant-Mbulu, Tanzania," *Innovative Energy and Research* 8, no. 225 (2019): 2.
[41] K. Kumar and R. P. Saini, "Data-Driven Internet of Things and Cloud Computing Enabled Hydropower Plant Monitoring System," *Sustainable Computing: Informatics and Systems* 36 (2022): 100823.
[42] A. Chanda, "Use of Arno Converter and Motor-Generator Set to Convert a Single-Phase AC Supply to a Three-Phase AC for Controlling the Speed of a Three-Phase Induction Motor by Using a Three-Phase to Three-Phase Cycloconverter," *International Journal of Electrical Engineering and Technology* 7, no. 2 (2016): 19–28.
[43] M. Musa, L. Ghobrial, C. Sasthav, et al., "Advanced Manufacturing and Materials for Hydropower: Challenges and Opportunities," (2023).
[44] E. Meli, R. Furferi, A. Rind, A. Ridolfi, Y. Volpe, and F. Buonamici, "A General Framework for Designing 3D

Impellers Using Topology Optimization and Additive Manufacturing," *IEEE Access* 8 (2020): 60259–60269.
[45] A. Z. Naser, I. Deiab, F. Defersha, and S. Yang, "Expanding Poly (Lactic Acid) (PLA) and Polyhydroxyalkanoates (PHAs) Applications: A Review on Modifications and Effects," *Polymers* 13, no. 23 (2021): 4271.
[46] A. Kawalec and M. Magdziak, "The Selection of Radius Correction Method in the Case of Coordinate Measurements Applicable for Turbine Blades," *Precision Engineering* 49 (2017): 243–252.
[47] G. Żywica, T. Z. Kaczmarczyk, Ł. Breńkacz, M. Bogulicz, A. Andrearczyk, and P. Bagiński, "Investigation of Dynamic Properties of the Microturbine With a Maximum Rotational Speed of 120 krpm–Predictions and Experimental Tests," *Journal of Vibroengineering* 22, no. 2 (2020): 298–312.
[48] M. M. Kamal, I. Ashraf, and E. Fernandez, "Optimal Sizing of Standalone Rural Microgrid for Sustainable Electrification With Renewable Energy Resources," *Sustainable Cities and Society* 88 (2023): 104298.